

# COMPUTATIONAL FRAMEWORK FOR DAMAGE MODELLING OF FIBER REINFORCED COMPOSITES

Michael Stuebner<sup>1</sup>, Endel V. Iarve<sup>2</sup>, Artëm Aleshin<sup>3</sup>, Eric G. Zhou<sup>4</sup>, David H. Mollenhauer<sup>5</sup>, Michael Braginsky<sup>6</sup>, and Brent L. Volk<sup>7</sup>

<sup>1</sup>University of Dayton Research Institute, Dayton, OH 45469, United States

Email: Michael.Stuebner@udri.udayton.edu, Web Page: <http://www.udri.udayton.edu>

<sup>2</sup>Department of Mechanical and Aerospace Engineering, The University of Texas at Arlington, 701 S. Neddeman Drive, Arlington, TX 76019

Email: Endel.Iarve@uta.edu, Web Page: <http://www.uta.edu/mae>

<sup>3</sup>Department of Mechanical Engineering, University of South Carolina, Columbia, SC 29208, United States

Email: Aleshin@email.sc.edu, Web Page: <http://www.me.sc.edu>

<sup>4</sup>University of Dayton Research Institute, Dayton, OH 45469, United States

Email: Eric.Zhou@udri.udayton.edu, Web Page: <http://www.udri.udayton.edu>

<sup>5</sup>Air Force Research Laboratory, Wright Patterson Air Force Base, OH 45433, United States

Email: David.Mollenhauer@us.af.mil, Web Page: <http://www.wpafb.mil/AFRL>

<sup>6</sup>University of Dayton Research Institute, Dayton, OH 45469, United States

Email: Michael.Braginsky@udri.udayton.edu, Web Page: <http://www.udri.udayton.edu>

<sup>7</sup>Air Force Research Laboratory, Wright Patterson Air Force Base, OH 45433, United States

Email: Brent.Volk.1@us.af.mil, Web Page: <http://www.wpafb.mil/AFRL>

**Keywords:** Fiber-reinforced composites, Laminates, Modeling, Damage

## Abstract

An advanced framework for damage modelling in composites applicable to a wide range of fiber reinforced polymer matrix and ceramic matrix composites is presented. The foundation for the framework is the finite element package BSAM designed at the University of Dayton Research Institute (UDRI). Several important generalizations make the package particularly suitable to advanced fracture simulations in composites: further improvements of discrete damage modelling capabilities, based on the Rx-FEM (regularized extended FEM) [1, 2], addition of the capability to perform geometrically nonlinear simulations, important for simulations of laminate structures and failure criteria, and incorporation of advanced tetrahedral elements, leading the way to robust modelling of textile composites.

## 1. Introduction

This paper is focused on the development of the suite of advanced modeling tools for performance evaluation and life prediction of a wide range of fiber reinforced polymer matrix and ceramic matrix composites. The development is a generalization of the general purpose finite element software package BSAM developed at the University of Dayton Research Institute (UDRI). The package is capable, in particular, to model laminates, advanced textile composites with structures provided by Virtual Textile Morphology Suite (VTMS) or taken from experiments. BSAM has extensive damage modelling capabilities, including discrete damage modelling based on the regularized extended FEM (Rx-FEM), [1,2], continuum damage, delaminations, etc.

Until recently, the code was capable of performing only geometrically linear FEM analysis. That led to limitations of its applicability to large deformation modeling of, for instance, beams and flanges, and, consequently, to simulating damage in such structures. The nonlinear analysis capability was implemented and validated with experimental data in collaboration with the University of South Carolina.

Another limitation of the code was its use of hexahedral elements only. These elements are very robust and powerful for simulations of the geometries that can be meshed. Unfortunately, many complex geometries, especially textile composites, cannot be fully meshed with hexahedral elements only. Even if a fully hexahedral mesh can be developed for some complex textile composite structure, the resulting mesh would have a huge number of elements with sizes that might span a couple of orders of magnitude making it not conducive for robust simulations. Tetrahedral elements have the advantage of being able to model complex geometries much better. However, the linear element (C3D4) has linear shape functions and only one integration point which makes it a constant strain/stress element – the reason those elements are never used in serious simulation work. The quadratic element (C3D10) with quadratic shape functions and 4 integration points is better suited to model deformation and damage. In order to simulate advanced textile composite materials, which improve damage tolerance and impact resistance of traditional laminates by implementing out-of-plane reinforcements, tetrahedral C3D10 elements have been added to the modeling toolbox of our framework.

## 2. Geometric nonlinear formulation

In finite element formulations it is usually assumed that the displacements are infinitesimally small, that the material is linearly elastic and that the boundary conditions remain unchanged. With these assumptions, the finite element equilibrium equations for static analysis form a linear system corresponding to a linear analysis of a structural problem. In many cases, these assumptions are not true anymore and a nonlinear analysis has to be performed. In contrast to linear elasticity, many different measures of strain and strain rate measures are used in nonlinear continuum mechanics. A strain measure must vanish for any rigid body motion, in particular for rigid body rotation. This is the key reason why the usual strain displacement equations are abandoned in nonlinear theory. In the following is a short description of the nonlinear methodology at the example of a total Lagrangian formulation, for details see [3, 4, 5]. It is assumed that the elementary particle occupies a position  $\mathbf{X}$  in space in the reference configuration (usually the undeformed configuration), with the so-called material coordinates  $(X_1, X_2, X_3)$ , and a position  $\mathbf{x}$ , with so-called spatial coordinates  $(x_1, x_2, x_3)$ , in the deformed configuration. Both are related through the displacement vector  $\mathbf{u}=(u_1, u_2, u_3)$ . Differentiating the spatial coordinates with respect to the material coordinates results in the deformation gradient  $\mathbf{F}$

$$\mathbf{F} = \frac{\partial \mathbf{x}}{\partial \mathbf{X}} = \frac{\partial x_i}{\partial X_j} = \mathbf{I} + \frac{\partial \mathbf{u}}{\partial \mathbf{X}} = \mathbf{I} + \frac{\partial u_i}{\partial X_j} . \quad (1)$$

A strain measure which fulfills this requirement is the Green-Lagrange strain  $\gamma$  which is defined as

$$\gamma_{ij} = \frac{1}{2} \left( \frac{\partial u_i}{\partial X_j} + \frac{\partial u_j}{\partial X_i} \right) + \frac{1}{2} \frac{\partial u_k}{\partial X_j} \frac{\partial u_k}{\partial X_i} . \quad (2)$$

The stress measure which is energetically conjugate to the Green–Lagrange strain tensor, is the Second Piola-Kirchhoff stress tensor  $\tau$

$$\tau_{ij} = \mathbf{D}\gamma_{ij} , \quad (3)$$

where  $\mathbf{D}$  is the material property tensor. For a quasi-static process the balance of momentum can be written as

$$\mathbf{f}^{\text{int}} = \mathbf{f}^{\text{ext}} \quad (4)$$

The internal forces  $\mathbf{f}^{\text{int}}$  in an element are given as

$$\mathbf{f}^{\text{int}} = \int_{V_0} \mathbf{B}^T \mathbf{t} \, dV \quad (5)$$

where  $\mathbf{B}$  is the element strain-displacement matrix and the external forces  $\mathbf{f}^{\text{ext}}$  depend on the loading and include cohesive forces. This leads to a system of nonlinear equations

$$\mathbf{F}(\mathbf{u}) = \mathbf{f}^{\text{int}}(\mathbf{u}) - \mathbf{f}^{\text{ext}}(\mathbf{u}) = 0. \quad (6)$$

A method to solve the system is the Newton-Raphson method. It requires the computation of the derivative of  $\mathbf{F}(\mathbf{u})$ . If the external forces do not change over time, then the derivative with respect to  $\mathbf{u}$  is zero. If they change, an appropriate formula for  $\frac{\partial \mathbf{f}^{\text{ext}}}{\partial \mathbf{u}}$  has to be applied. For the internal forces one obtains after some derivation and linearization

$$\frac{\partial \mathbf{f}^{\text{int}}}{\partial \mathbf{u}} \approx \mathbf{K}_T = \mathbf{K}_L + \mathbf{K}_{NL} = \int_{V_0} \mathbf{B}_L^T \mathbf{D} \mathbf{B}_L \, dV + \int_{V_0} \mathbf{B}_{NL}^T \mathbf{T} \mathbf{B}_{NL} \, dV \quad (7)$$

Where  $\mathbf{K}_T$  is the tangent stiffness matrix which consists of two parts, the material tangent stiffness matrix  $\mathbf{K}_L$  which depends on the material response and the geometric stiffness  $\mathbf{K}_{NL}$  which accounts for geometric effects of the deformation.  $\mathbf{B}_L$  is the element strain-displacement matrix to which the deformation gradient is applied to,  $\mathbf{B}_{NL}$  a matrix of derivatives of shape functions and  $\mathbf{T}$  the second Piola-Kirchhoff stress tensor, see for instance [4] for their exact definitions. The iteration formula is then given as

$$\mathbf{u}_{i+1} = \mathbf{u}_i - \mathbf{K}_T^{-1} (\mathbf{f}_i^{\text{int}} - \mathbf{f}_i^{\text{ext}}) \quad (8)$$

and is executed until convergence is achieved.

### 3. Validation of the nonlinear implementation

#### 3.1. Hexahedral elements (C3D8)

To validate and evaluate the nonlinear modeling capabilities of BSAM with respect to compression bending, experiments and simulations were conducted at the University of South Carolina (USC) in collaboration with the Air Force Research Laboratory (AFRL).

The experimental data for the compression bending phenomena was acquired at USC with the use of two Three-Dimensional Digital Image Correlation systems (to measure the strains on the compression and tension sides), a Tinius Olsen Material Testing System (MTS), and two custom made specimen grips which provided the specimen with the ability to bend out of plane during axial displacement. The material used for the testing, an eight layer zero degree unidirectional composite layup (IM7/977-3), was provided by AFRL. The specimen (Fig. 1) having a width of one inch, length of six inches and thickness of one millimeter, was tested in compression bending up to the point of catastrophic failure.

Two separate geometry and finite element models were created for simulating the composite specimen in compression loading, with the former model having fewer elements through the thickness, but more elements along the width of the specimen. Furthermore, the latter model was the one predominantly used for validation. Both models were created with Gmsh, an open source finite element mesh generator, which was used to accurately model the specimen dimensions and to discretize the geometry into standard eight-node brick elements.

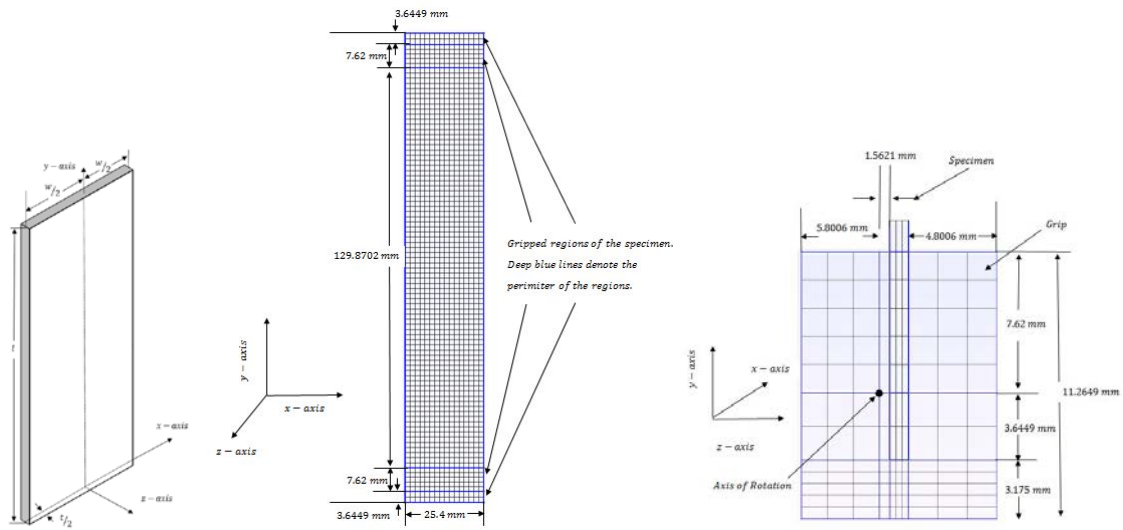


**Figure 1.** Dimensions and coordinate system for unidirectional composite specimen geometry (left), front (middle) and side view of meshed specimen and grip (right).

The model was setup to run with various iteration steps. A graph comparing the experimental and computed (using 100 and 200 iteration simulations) maximum out of plane displacements as a function of the displacement of the top grip is given in Fig. 2, demonstrating that there is virtually no difference in displacement computation between 100 and 200 step simulations. Furthermore, the figure shows that the modeled displacements reflect the experimental ones extremely well.

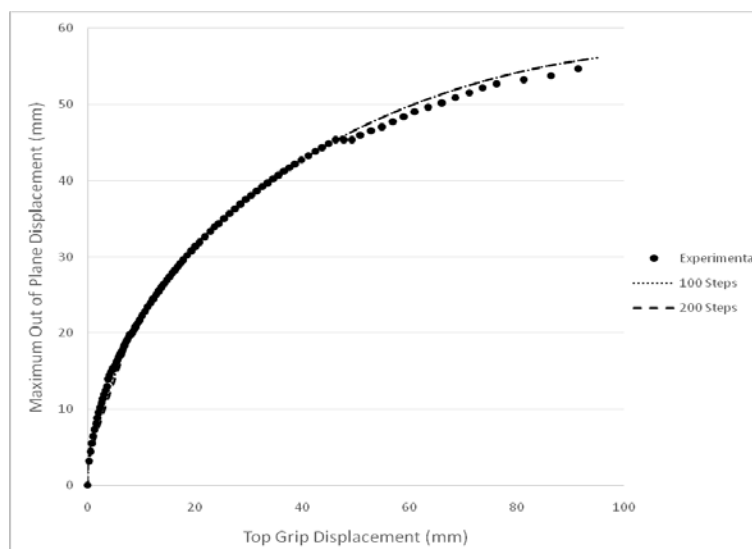


**Figure 2.** Comparison of maximum out of plane displacement results.

The maximum axial strains obtained through the simulation were compared to those measured during the experiment. Graphs comparing the absolute maximum and minimum strains on the compression and tension sides are provided in Fig. 3 and 4, respectively. The combined results given in Fig. 2, 3, 4 and 5 demonstrate that the nonlinear implementation in BSAM can accurately predict the maximum displacements and strains experienced by a specimen undergoing compression bending.

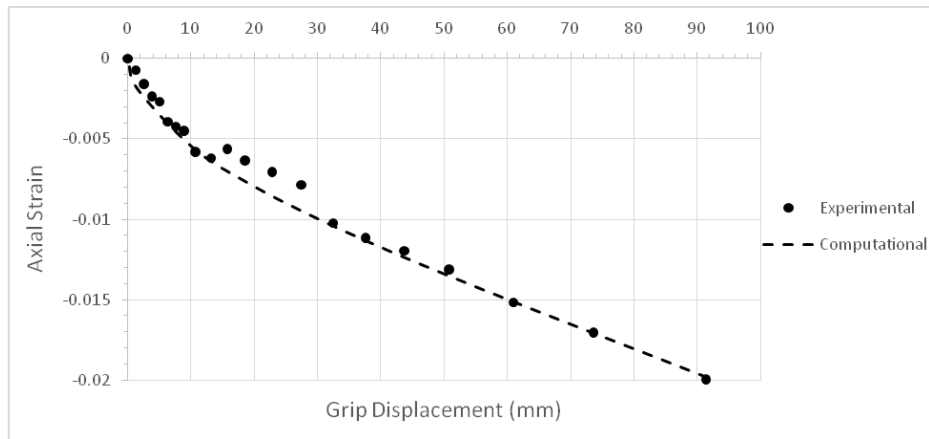


**Figure 3.** Comparison of experimental and computational axial strain at the center of the compression side of the specimen, ( $w/2, l/2, -t/2$ ).

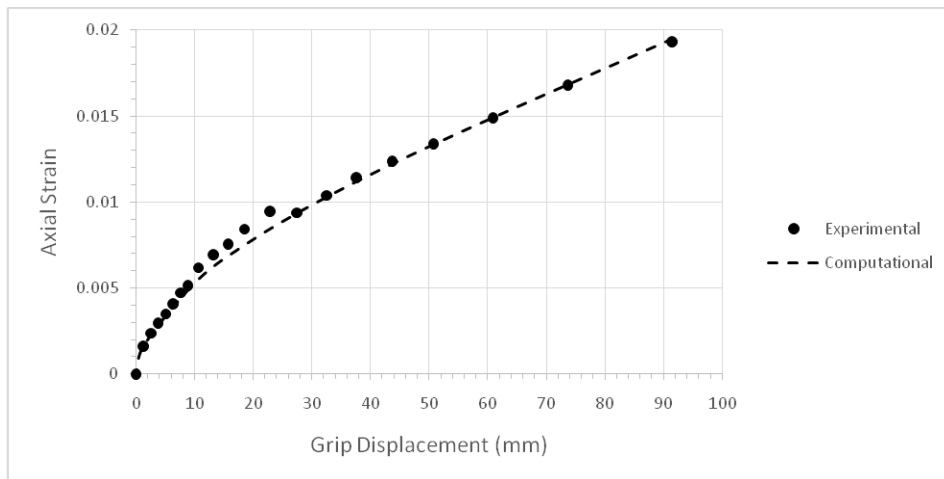


**Figure 4.** Comparison of experimental and computational axial strain at the center of the tension side of the specimen, ( $w/2, l/2, t/2$ ).

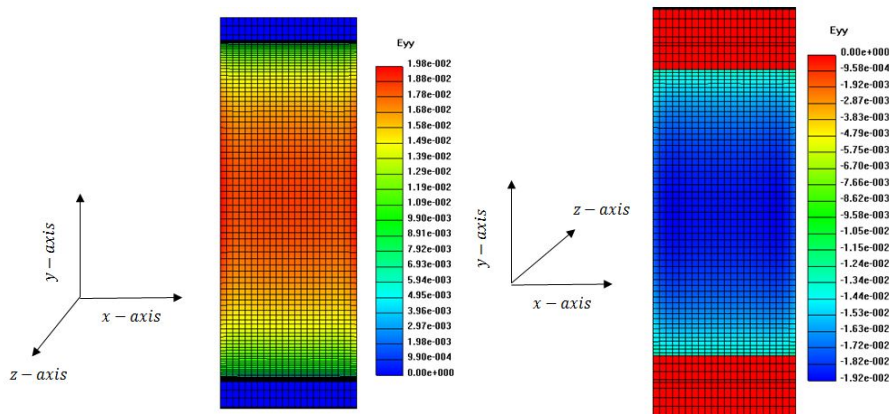


**Figure 5.** Axial strain on the tension side ( $t/2$ ) (left) and compression side ( $-t/2$ ) (right) of the specimen at a load of 90 mm.

### 3. Validation of the non-linear implementation using quadratic tetrahedral elements (C3D10)

As stated above, tetrahedral elements have the advantage of being able to model complex geometries much better. Therefore, quadratic element (C3D10) with quadratic shape functions and 4 integration points has been implemented into the modelling framework. The example below shows validation of the element implementation together with the illustration of the importance of incorporating of geometric nonlinearity into simulations of laminate parts.

Fig. 6 below shows different stages of deformation of a 4-ply laminate unidirectional composite layup (IM7/8552) with 0/45/0/-45 stacking sequence subjected to compression loading in nonlinear (Fig. 6, left column) and linear (Fig. 6, right column). One side of the plate perpendicular to the x-axis is fixed while displacement is prescribed on the other.

With a small displacement applied, the first row in the table, nonlinear and linear simulations give very similar results, as expected. As load increases, the nonlinear and linear simulation results diverge, and at 10% strain shown in the second row in Fig. 6, they clearly are not even close. While this simulation does not include failure, these results clearly show that, damage in linear and nonlinear simulations cannot be identical or, indeed, even close, since failure criteria involve stress/strain fields.

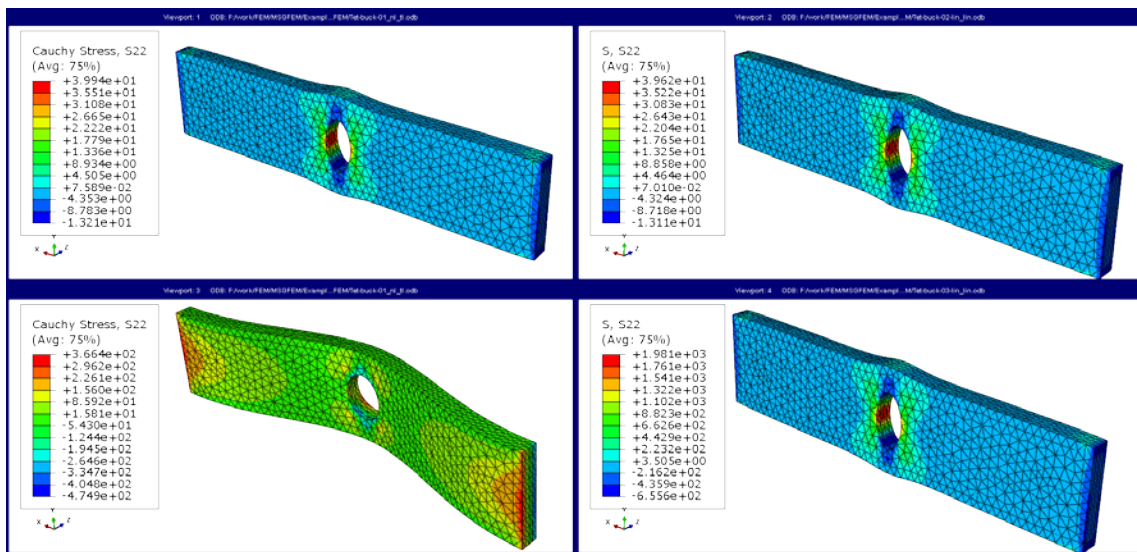


**Figure 6.** Stress for an OHC run modeled with nonlinear (left) and linear quadratic tetrahedral elements for small displacement (top) and larger displacement (bottom) applied.

### 4. Conclusions

Significant improvements to the general finite element package BSAM particularly suitable for advanced fracture simulations of composites have been demonstrated and validated. Those important improvements include the added ability to simulate large deformations via geometrically nonlinear approach and the addition of higher order tetrahedral elements leading to increased capability for robustly modelling stress/strain state and damage in complex, especially textile, composite structures.

### Acknowledgments

The work is supported by the Air Force Research Laboratory under University of Dayton Research Institute Contract FA8650-10-D-5011.

## References

- [1] E.V. Iarve (2003) Mesh independent modelling of cracks by using higher order shape functions, *Int. J. Numer. Meth. Engng*, **56**, 869-882.
- [2] E.V. Iarve, M.R. Gurvich, D.H. Mollenhauer, C.A. Rose, and C.G. Davila (2011) Mesh-independent matrix cracking and delamination modeling in laminated composites. *Int. J. Numer. Meth. Engng*, **88**, 749–773.
- [3] H. Belytschko, W.K. Liu, and B. Moran. *Nonlinear Finite Elements for Continua and Structures*. John Wiley & Sons, Ltd., 2001.
- [4] R. de Borst, M. A. Crisfield, J.J.C. Renner and C.V. Verhoosel. *Non-linear Finite Element Analysis of Solids and Structures*. John Wiley & Sons, Ltd., 2012.
- [5] K.J. Bathe. *Finite Element Procedures*. Prentice Hall, 1996.